Photoproduction of $\Theta^+(J^P = 3/2^\pm)$ from the proton and neutron

Seung-Il Nam[1], Atsushi Hosaka[2] and Hyun-Chul Kim[1]
[1]*Department of Physics and Nuclear physics & Radiation Technology Institute (NuRI) Pusan National University, Busan 609-735, Korea*
[2]*Research Center for Nuclear Physics (RCNP), Osaka University, Ibaraki, Osaka 567-0047, Japan*

1 Introdution

Since Diakonov *et al.* predicted the mass and width of the pentaquark baryon Θ^+ [1], there has been a great deal of works to clarify its existence and properties. Although various experiments have reported the existence of Θ^+ after the first observation by the LEPS collaboration [2], the situation is not yet settled down primarily due to the relatively low statistics of the low-energy experiments. Furthermore, in almost all high-energy experiments, the Θ^+ has not been seen (see, for example, a recent review [3, 4, 5] for the compilation of the experimental results).

Recently, the CLAS collaboration has reported null results for finding the Θ^+ in the reactions $\gamma p \to \bar{K}^0 K^+ n$ [6]. A preliminary results of no evidence from the deuteron experiment has been also reported. The upper limit of the cross section of producing Θ^+ was estimetaed to be $\sigma(\gamma p \to \bar{K}^0\Theta^+) \sim 0.8$ nb. Though these experiments had high statistics, their results do not yet lead to the absence of Θ^+ immediately, because the updatd positive evidences also seem rather convincing. In the LEPS, they observe a peak for the Θ^+ in the reaction $\gamma d \to \bar{\Lambda}(1520) n K^+$ [7] when the $\Lambda(1520)$ is detected in the forward angle region.

Experimentally, the two similar experiments from CLAS and LEPS are not in contradiction, since they measure different regions; CLAS detects produced particles in a large angle (side) region, while the LEPS observes the small angle (forward) region, and their measuring regions have little overlap.

In the present work, we would like to provide a mechanism for the strong suppression of the reaction process $\gamma p \to \bar{K}^0\Theta^+$, as compared to $\gamma n \to K^-\Theta^+$. A similar result has been obtained in the recent work for $\Lambda(1520, J^P = 3/2^-)(\equiv \Lambda^*)$ photoproduction [8], where we have shown the strong suppression of the charge non-exchange channel; $\sigma_{\gamma n \to K^0\Lambda^*} \ll \sigma_{\gamma p \to K^+\Lambda^*}$. The large difference between the two reactions was caused by the dominant contribution from the contact (Kroll-Ruderman like) term.

We employ the effective Lagrangian method, where the Born terms as shown in Fig. 1 are calculated. Here we can make some theoretical constraints from the low energy side. Within a reasonable model setup, we show a remarkable role of the contact term for the neutron targets for $\Theta^+(J^P = 3/2^\pm)$, which is, however, absent for the proton target. An advantage of the spin 3/2 states especially with the negative parity is in that that state is compatible with the very narrow width; in the quark model picture, the simple configuration $(0s)^5$ forbids the decay into the KN state in the d-wave [9].

Figure 1: Born diagrams calculated in the effective Lagrangian method.

2 Formalism

Let us start with a brief description of the effective Lagrangian method. The spin 3/2 particle is treated in the Rarita-Schwinger formalism. Then the basic symmetries such as Lorentz covariance and gauge symmetry enable one to write the interaction Lagrangians as follows:

$$\begin{aligned}
\mathcal{L}_{\gamma NN} &= -e\bar{N}\left[\not{A} + \frac{\kappa_p}{2M_p}\sigma_{\mu\nu}F^{\mu\nu}\right]N + \text{h.c.},\\
\mathcal{L}_{\gamma KK} &= ie\left[(\partial^\mu K^\dagger)K - (\partial^\mu K)\,K^\dagger\right]A_\mu,\\
\mathcal{L}_{\gamma\Theta\Theta} &= e\bar{\Theta}^\mu\left[\not{A} + \frac{\kappa_\Theta}{2M_\Theta}\sigma_{\nu\rho}F^{\nu\rho}\right]\Theta_\mu + \text{h.c.},\\
\mathcal{L}_{\gamma KK^*} &= g_{\gamma KK^*}\epsilon_{\mu\nu\sigma\rho}(\partial^\mu A^\nu)(\partial^\sigma K)K^{*\rho} + \text{h.c.},
\end{aligned}$$

$$
\begin{aligned}
\mathcal{L}_{KN\Theta} &= \frac{g_{KN\Theta}}{M_K}\bar{\Theta}^\mu \partial_\mu K \Gamma_5 N + \text{h.c.}, \\
\mathcal{L}_{K^*N\Theta} &= -\frac{ig_{K^*N\Theta}}{M_V}\bar{\Theta}^\mu \gamma^\nu [\partial_\mu K^*_\nu - \partial_\nu K^*_\mu]\Gamma_5\gamma_5 N + \text{h.c.}, \\
\mathcal{L}_{\gamma KN\Theta} &= -ie\frac{g_{KN\Theta}}{M_K}\bar{\Theta}^\mu A_\mu K \Gamma_5 N + \text{h.c.},
\end{aligned} \tag{1}
$$

where N, Θ^μ, K and A^μ are the nucleon, $\Theta^+(3/2^\pm)$, pseudoscalar kaon and photon fields, respectively, and $\Gamma_5 = 1$ for $\Theta^+(3/2^+)$, while $\Gamma_5 = \gamma_5$ for $\Theta^+(3/2^-)$. Note that the meson-baryon couplings here are constructed in the pseudovector (PV) scheme with the derivative acting on the kaon field. For the spin 3/2 case, this is the natural method to introduce the meson-baryon couplings including Θ^+. Therefore, we need to have the contact term as in Eq. (1) explicitly.

In Eq. (1), various coupling constants are introduced with obvious notation. As for the electric part of the $\gamma\Theta\Theta$ vertex, we consider only the $g_{\mu\nu}$ term from Eq. (5) of Ref. [10]: $e\Theta^\mu \not{A}\Theta_\mu$. Hence, the propagator of $\Theta^\mu(3/2^\pm)$ is approximated to take the form of spin-1/2 fermion. In fact, we have verified that the approximation works well since the relevant u-channel contribution is strongly suppressed by the form factor. For the decay width of Θ^+, we choose $\Gamma_{\Theta\to KN} = 1$ MeV [11, 12]. This choice gives $g_{KN\Theta} = 0.53$ for $\Theta^+(3/2^+)$ and $g_{KN\Theta} = 4.22$ for $\Theta^+(3/2^-)$. The unknown parameter $g_{K^*N\Theta}$ is estimated by the quark model. As for $\Theta^+(3/2^+)$ we employ the relation $|g_{K^*N\Theta}| = \sqrt{3}g_{KN\Theta}$ [16], which is applicable to both $1/2^+$ and $3/2^+$ states. On the other hand, we find $|g_{K^*N\Theta}| \sim 2$ for $\Theta^+(3/2^-)$ of $(0s)^5$ configuration. In numerical calculation, we test the values of $\pm|g_{K^*N\Theta}|$ and 0 in order to see the role of K^*.

As for the form factor, we employ the four dimensional gauge and Lorentz invariant one which was used in Ref. [8]. There, it was shown that this form factor with the cutoff $\Lambda = 750$ MeV reproduced experimental data of the photoproduction of $\Lambda(1520)$ [8] qualitatively well. As for the anomalous magnetic moment of Θ^+, we choose $\kappa_\Theta = 1$, which is an upper bound among the existing estimation. In the quark model calculation, its value is very small if Θ^+ has $J^P = 3/2^-$ [8]. The resulting amplitude, however, does not depend much on κ_Θ, since the form factor suppresses the s- and u-channel contributions that are proportional to κ_Θ. Since the calculation of the Born terms for $\Theta^+(3/2^\pm)$ photoproduction is analogous to that of Λ^*, we refer to Ref. [8] for details.

3 $\Theta^+(3/2^\pm)$

Let us now discuss our results. First, we show various contributions to the total cross section in Fig. 2, where results are shown separately as functions of the incident photon energy E_γ for the s-, t-, u-channels, K^*-exchange and the contact term for the neutron target, and for s-, u-channels, and K^*-exchange for the proton. It is shown that the largest contribution is from the contact term which is present only for the neutron, while the u- and s-channel contributions are strongly suppressed due to the form factor. This is so because the baryon in the u- and s-channels are further off mass shell than in the t-channel. The K^*-exchange contributes some, but the amount is significantly smaller than that of the contact term. From these observations, we expect that whether the contact term is present or not yields the large difference in the production rates from the proton and neutron targets.

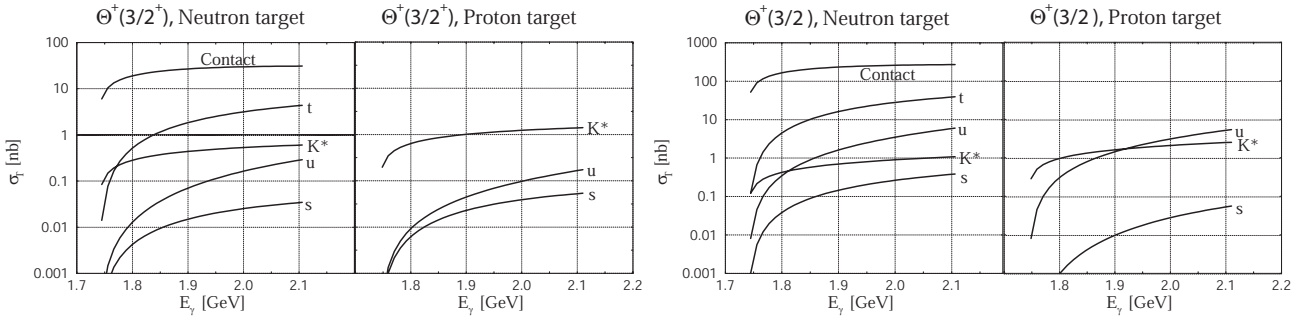

Figure 2: Total cross sections for each kinematical channel for $J^P = 3/2^+$ (upper two panels) and for $J^P = 3/2^-$ (lower two panels). Here, we use $\Gamma_{\Theta\to KN} = 1.0$ MeV. $g_{K^*N\Theta} = +0.91$ for the positive parity and $+2$ for the negative one.

We can verify this explicitly as shown in the upper two panels of Fig. 3, where the total cross sections including all kinematical channels are plotted in logarithmic scale for $J^P = 3/2^+$ (left panel) and $3/2^-$ (right panel), and for proton (dashed lines) and neutron (solid lines). Three curves are obtained by using different

values of $g_{K^*N\Theta}$ as indicated in the figures. As anticipated, the contact term is dominant for the neutron target, which makes the cross sections significantly larger than for the proton target. The cross sections averaged in the energy range $1.73 < E_\gamma < 2.10$ GeV are summarized in Table 1. The numerical values are evaluated when $|g_{K^*N\Theta}| = 0.91 (J^P = 3/2^+)$ and 2 $(J^P = 3/2^-)$; they do not depend much on the sign of the coupling constant as we can see from Fig. 3. We find that the Θ^+ production rate is larger for the neutron than for the proton, when the above finite values are used for $g_{K^*N\Theta}$, by factors $\sim 25\,(3/2^+)$ and $\sim 50\,(3/2^-)$. If $g_{K^*N\Theta} = 0$, the difference is even more enhanced.

Absolute values are larger for the negative parity than for the positive parity, due to the large difference in the coupling constant; $g_{KN\Theta}(J^P = 3/2^+) = 0.53$ and $g_{KN\Theta}(J^P = 3/2^-) = 4.22$. This difference stems from the different coupling structure of Θ^+ to the decaying KN channel, p-wave for $3/2^+$ and d-wave for $3/2^-$ [13].

Once again we note that these cross sections are computed using the parameters corresponding to $\Gamma_{\Theta\to KN} = 1.0$. For other values of $\Gamma_{\Theta\to KN}$, they are precisely proportional to $\Gamma_{\Theta\to KN}$ for $3/2^+$, while it is approximate for $3/2^-$.

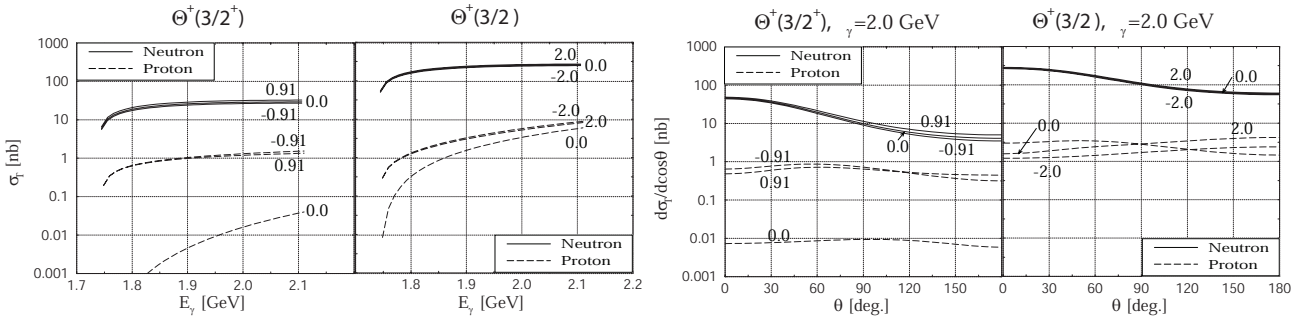

Figure 3: Upper two panels: Total cross sections for $J^P = 3/2^+$ (left) and for $J^P = 3/2^-$ (right). Lower two panels: Differential cross sections for $J^P = 3/2^+$ (left) and for $J^P = 3/2^-$ (right). The numbers on the figures denote the values of the coupling constant $g_{K^*N\Theta}$.

In the lower two panels of Fig. 3 we present the differential cross sections when $E_\gamma = 2.0$ GeV. For the neutron target we observe strong forward enhancement, which is the characteristic feature of the contact term with the gauge invariant form factor. On the contrary, for the proton target a bump appears at around 60° when K^*-exchange is present; the angle dependence of the $K^*N\Theta$ coupling characterizes it. If the K^*-exchange is absent, the cross section is backward peak which is the character of the u-channel process. These different angular distributions may help understand the production mechanism of Θ^+.

4 $\Theta^+(1/2^+)$

Now it is interesting to compare the above results of $J^P = 3/2^\pm$ with those of $J^P = 1/2^+$. Here we assume the positive parity, since the negative parity is not likely to be compatible with the narrow decay width [9]. The reaction for the Θ^+ of $J^P = 1/2^+$ has been investigated previously and we refer to Refs. [14, 15] for details. An important fact for the case of $J^P = 1/2^+$ is that one can construct the effective Lagrangians both in the pseudoscalar (PS) and in the pseudovector (PV) schemes. In a consistent description, these two schemes should be equivalent in the strong interaction sector. In fact, it was shown explicitly that the difference between the two schemes are due to the terms of anomalous magnetic moments which is the electromagnetic coupling [14, 15]. Hence for the computation of cross sections we shall work out in the PS scheme with using the four dimensional form factor. To make our comparison fair, we adopt the parameters reproducing $\Gamma_{\Theta\to KN} = 1.0$ MeV [12] which gives $g_{KN\Theta} = 1.0$ and $|g_{K^*N\Theta}| = \sqrt{3} g_{KN\Theta} = 1.73$. For the magnetic moment we have used $\kappa_\Theta = 1$ again.

In the left panel of Fig. 4, we show the total cross sections as functions of E_γ, where we show the results with $g_{K^*N\Theta} = 0$ and $+1.73$. The result with $g_{K^*N\Theta} = -1.73$ is qualitatively similar to that of $g_{K^*N\Theta} = +1.73$. When $g_{K^*N\Theta}$ has a sizable value ($g_{K^*N\Theta} = +1.73$), the total cross sections for the two different targets do not show obvious differences. On the other hand, the production rate is suppressed by a factor $\lesssim 5$ for the proton target, when K^*-exchange is absent. In both cases the cross sections of the proton is less suppressed as compared to the neutron, a feature which is different from the case of $\Theta^+(J^P = 3/2^\pm)$. We can understand this from the different role of the contact term. To this end, we consider the results in the PV scheme, where the contact term appears necessarily. For $J^P = 1/2^+$, the gauge invariance and the equivalence between the PS and PV schemes requires that the form factor of the contact term must be the same as for the u-channel. Consequently, the contributions of the u-channel and contact term are similar. In contrast, for the spin 3/2 cases where only the PV scheme is available, the contact term remains dominant.

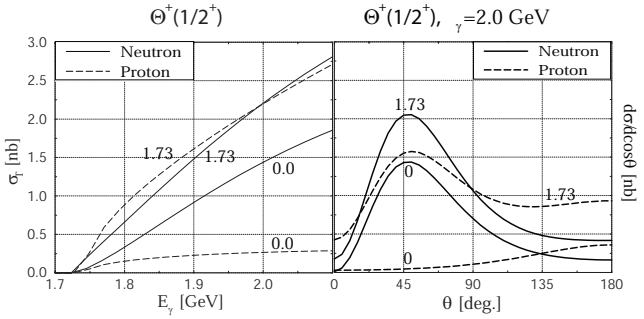

Figure 4: Total (left) and differential (right) cross sections for $\Theta^+(1/2^+)$. The numbers on the figures denote the values of the coupling constant $g_{K^*N\Theta}$.

The differential cross sections at $E_\gamma = 2.0$ GeV are shown in the right panel of Fig. 4. In three cases curves show a bump at around 45°, which is a feature of both the K-exchange and K^*-exchange terms. Only when both of them are absent (for the proton without K^*), the bump structure disappears, where instead, the backward peak appears as is the property of the u-channel contribution. These angular distributions are once again very much different from the case of $J^P = 3/2^\pm$ in particular for the neutron target.

5 Summary and Conclusion

In this work, we have studied the photoproduction of Θ^+ for $J^P = 3/2^\pm$ and $1/2^+$, where we have computed the Born diagrams using the effective Lagrangians. The gauge and Lorentz invariant four dimensional form factor was employed with the cutoff determined to reproduce the data of the $\Lambda(1520)$ photoproduction [8]. Several unknown parameters were estimated by the quark model and some phenomenological considerations.

We have then found that the production rate for the proton target is significantly suppressed as compared to that of the neutron. This result is governed by the contact term which is present only in the charge exchange process for the neutron target. A similar observation was made in the previous study of the photoproduction of $\Lambda(1520)$, where the role of the proton and neutron was interchanged. The present result was obtained by fixing several parameters in an expectedly reasonable manner, especially by using the form factors determined in the phenomenological analysis of the $\Lambda(1520)$ photoproduction, hoping that the form factors for Θ^+ and $\Lambda(1520)$ are not very much different. However, the difference in the $\Lambda(1520)$ production rates between the proton and neutron targets are not yet measured in experiment. It is therefore very important to check this in the future experiments.

In Table 1, we summarize and compare various cross sections averaged in the energy range $1.73 < E_\gamma < 2.10$ GeV. From the table, in all cases, the cross sections for the proton target are of order of a few nb. Interestingly, these values seem compatible with the upper bound, if Θ^+ exists, as extracted from the recent CLAS experiment [6]. Therefore, one of our conclusions is that the results of the CLAS does not immediately lead to the absence of Θ^+. Our present study have shown that the photoproduction of Θ^+ could be suppressed for the proton target. In contrast, the cross sections are sizable for the neutron target as large as 25 nb ($J^P = 3/2^+$) and 200 nb ($J^P = 3/2^-$), when $\Gamma_{\Theta\to KN} = 1$ MeV is employed. Furthermore, even for the neutron target, the angular dependence is highly forward peaking when $E_\gamma \gtrsim 2$ GeV. Therefore, unless the experimental detecter is located in the forward angle region, they would miss a large part of the total cross sections. This could explain the different results from LEPS and CLAS. It would be desired to perform consistently at a single facility the observation in a wide angle region.

J^P	$3/2^+$		$3/2^-$		$1/2^+$	
$g_{KN\Theta}$	0.53		4.22		1.0	
$g_{K^*N\Theta}$	± 0.91		± 2		± 1.73	
Target	n	p	n	p	n	p
σ	~ 25 nb	~ 1 nb	~ 200 nb	~ 4 nb	~ 1 nb	~ 1 nb
$\frac{d\sigma}{d\cos\theta}$	Forward	$\sim 60°$	Forward	–	$\sim 45°$	$\sim 45°$

Table 1: Main results of the Θ^+ photoproduction, where all results are for the case of finite $g_{K^*N\Theta}$.

We are very grateful to J. K. Ahn, K. Hicks, T. Hyodo, T. Nakano, A. Titov and H. Toki for fruitful discussions. The work of S.I.N. has been supported by the scholarship from the Ministry of Education, Culture, Science and Technology of Japan. The work of A.H. is also supported in part by the Grant for Scientific Research ((C) No.16540252) from the Education, Culture, Science and Technology of Japan. The works of H.C.K. and S.I.N. are supported by the Korean Research Foundation (KRF–2003–070–C00015).

References

[1] D. Diakonov, V. Petrov and M. V. Polyakov, Z. Phys. **A359**, 305 (1997).

[2] T. Nakano *et al.* [LEPS Collaboration], Phys. Rev. Lett. **91**, 012002 (2003).

[3] K. Hicks, arXiv:hep-ex/0504027.

[4] R. A. Schumacher, nucl-ex/0512042.

[5] K. H. Hicks [CLAS Collaboration], hep-ex/0510067.

[6] M. Battaglieri *et al.* [CLAS Collaboration], Phys. Rev. Lett. **96**, 042001 (2006).

[7] T. Nakano, For instance, talk given at the workshop Pentaquark05, J-Lab, October 20-22, 2005.

[8] S. I. Nam, A. Hosaka and H. -Ch. Kim, arXiv:hep-ph/0503149.

[9] A. Hosaka, M. Oka and T. Shinozaki, Phys. Rev. D **71**, 074021 (2005).

[10] B. J. Read, Nucl. Phys. B **52**, 565 (1973).

[11] T. Hyodo and A. Hosaka, Phys. Rev. D **71**, 054017 (2005).

[12] S. Eidelman *et al.* [Particle Data Group], Phys. Lett. B **592**, 1 (2004).

[13] X. G. He, T. Li, X. Q. Li and C. C. Lih, Phys. Rev. D **71**, 014006 (2005).

[14] S. I. Nam, A. Hosaka and H. -Ch. Kim, Phys. Lett. B **579**, 43 (2004).

[15] S. I. Nam, A. Hosaka and H. -Ch. Kim, arXiv:hep-ph/0403009.

[16] F. E. Close and J. J. Dudek, Phys. Lett. B **586**, 75 (2004).